Human-Arm Roll Estimation in Underactuated Grippers with Proprioceptive Feedback

Juan M. Gandarias, Francisco Pastor, Antonio J. Muñoz-Ramírez, and
Jesús M. Gómez-de-Gabriel, *Member, IEEE*

***Abstract*— In this paper, a method for the estimation of the roll angle of a human forearm, when grasped by a robot with an underactuated gripper, using proprioceptive information only, is presented. A common place to handle a human arm is by the distal forearm, just before the wrist. Knowing the angle around the forearm's axis (i.e. roll angle) is key for the safe manipulation of the human limb and biomedical sensor placement among others. The adaptive gripper has two independent underactuated fingers with two phalanges and a single actuator each. The final joint position of the gripper provides information related to the shape of the grasped object without the need for external contact or force sensors. Regression methods to estimate the roll angle of the grasping have been trained with forearm grasping information from different humans at each angular position. The results show that it is possible to accurately estimate the rolling angle of the human arm, not only for known people but also for humans for which haven't been previously trained. With this method, new applications of robot-initiated pHRI (Physical Human-Robot Interaction) can be developed without the need for external force/tactile sensors.**

I. Introduction

The two-way physical interaction with robots may help people in multiple ways. It has been demonstrated that the use of interactive robots enhances people's mood and raises the communication frequency [1]. Moreover, in [2] the effects of hugging robots on the social behaviour of people is presented, having found improvements where people have been hugged by a robot compared to the results of people that hugged robots.

Despite the fact that the applications where robots are able to manipulate people are very interesting for robotics researchers, there are few studies that consider direct human-robot physical contacts. Most researches carried out that are related to physical Human-Robot Interaction (pHRI) consist of control techniques of teleoperated systems [3], exoskeletons [4], prosthetic parts or rehabilitation robots [5].

Regarding these few pHRI applications, a robot that cleanses human limbs of disabled people is presented in [6] and a robot that manipulates human limbs with a non-prenssil actuator and an impedance Model Predictive Control (MPC) is presented in [7]. More recent studies have considered the application of artificially intelligent techniques for robotically assisted dressing [8].

Fig. 1. Manipulator with adaptive gripper for robot-initiated human interaction.

One aspect that has to be addressed in pHRI refers to robotics grippers. Although multiple ad-hoc end-effectors have been considered in previous pHRI works [9], it is still necessary to develop grippers or hands that allow the robot to carry out autonomous and safe grasps [10], with enough robustness and softness to manipulate human limbs. Some studies about pHRI grippers are based on the use of Variable Stiffness Actuators (VSA) [11], and the integration of tactile sensors and deep learning methods in robotic grippers to distinguish contacts with humans and inert objects is presented in [12].

The use of adaptive or flexible grippers enhance the in-hand manipulation by reducing the maximum pressure applied over the grasped objects [13]. However, the precision of this kind of mechanism is lower than in rigid grippers. Other existing solutions are based on underactuated rigid hands that adapt their shape over the contact surface. The underactuated and fully rigid PaCome gripper [14], originally thought for industrial applications, could also be used for pHRI applications. In [15], OpenHand is presented. It is an hybrid rigid-soft and open hardware gripper made of 3D printed polylactic acid (PLA) and polyurethane rubber. In a

This work was supported by the the Spanish project DPI2015-65186-R and the European Commission under grant agreement BES-2016-078237, and Universidad de Mlaga. Campus de Excelencia Internacional Andaluca Tech.

J.M. Gandarias, F. Pastor, A.J. Muñoz-Ramírez, A.J. García-Cerezo and J.M. Gómez-de-Gabriel are with the Telerobotics and Interactive Systems Laboratory (TaIS Lab), Systems Engineering and Automation Department, University of Málaga. Escuela de Ingenierías Industriales, Málaga, Spain. E-mail: jmgandarias@uma.es

TABLE I

PARAMETER VALUES OF THE UNDERACTUATED FINGER.

Parameter	Value	Parameter	Value
$\overline{O_1O_a}$	$[16,-20]$ mm	c	20 mm
L_0, L_1, L_2	40 mm	d	8 mm
a	25 mm	ψ	90°
b	60 mm	width	15 mm

recent study of the same authors, proprioceptive and tactile information are combined to classify grasps with a hybrid underactuated gripper [16].

In this paper, the problem of human forearm manipulation is addressed. To face this problem, a gripper with two independent underactuated fingers has been designed and built using additive manufacturing technology. Each finger has two phalanx, a single motor and an angle sensor placed in the underactuated joint. Using these sensors and the actual position angle given by the motors, a robot could have this proprioceptive information which allows the estimation of shape and size of the in-hand object. The main contribution of this study is to solely use the proprioceptive information given by the angle sensors integrated in the gripper to grasp the distal forearm and estimate the roll angle using machine learning approaches based on non-linear regression methods. Therefore, to the best of our knowledge, this is the first work in which the human-robot interaction is carried out, being directly initiated by the robot. According to this study, a robot manipulator with an underactuated gripper could grasp a distal forearm and estimate the grasping roll angle using haptic feedback only, which could open the door to new research lines into safety human manipulation.

This paper is structured as follows: In section II the designed prototype of the underactuated gripper and its validation is presented. In section III, the new method developed for the estimation of the forearm roll angle, based on machine learning techniques is then described, and the conclusions are shown in section IV.

II. ADAPTIVE GRIPPER

There are two main approaches for the implementation of the driving mechanism: tendons and rigid linkages [17]. In this application, the use of tendons (e.g. Yale OpenHand Model T42), as in [15] has been discarded, because the tendons are located in the internal side of the fingers, increasing the size of parameter d so the contact surfaces of the fingers pinch the skin of the forearm. However, the linkages are located on the back of the finger, leaving a cleaner contact area.

A. Kinematics

A gripper with two independent underactuated fingers with two phalanx and a single actuator has been designed with the kinematic described in Figure 2. The parameter values, summarised in Table I, have been designed to adapt to the shape and size of a human upper-forearm with a perimeter between 15.3 and 18.8 cm.

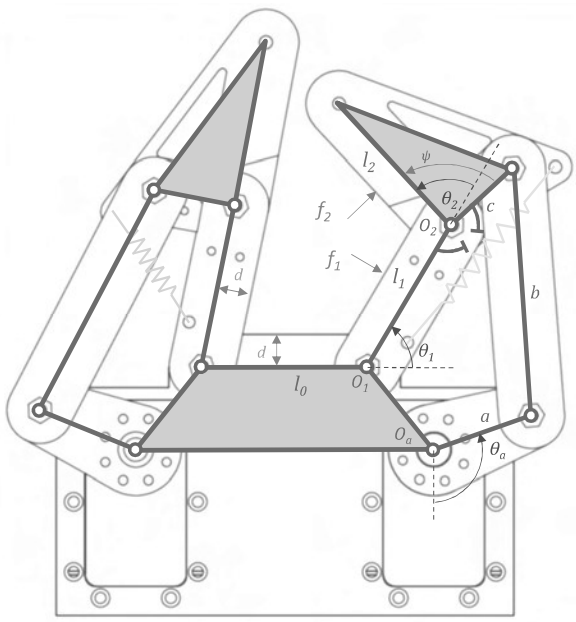

Fig. 2. Kinematic of the underactuated fingers. Each finger is independent, with two DOF's (θ_1,θ_2) and a single actuator θ_a. A mechanical stop makes $\theta_2 > 0$. The actual position of the finger depends on the external forces f_1, f_2 and the actuator torque. A spring ensures contact between the finger pads and external objects

A mechanical limit makes the distal phalanx angle θ_2 always positive. The actual position of the finger depends on the balance between external forces f_1, f_2 and the actuator torque. The spring ensures contact between the finger pads and external objects and make the finger stable when f_1 or f_2 are 0. The extension springs are made with $0.6mm\oslash$ steel wire and a stiffness of 164N/m.

The prototype has been manufactured in PLA plastic in a *Prusa MK2* 3D-printer, and its design has been made freely accessible in a public repository [1].

B. Proprioceptive sensing

Analog angle sensors have been placed to measure the distal joint angles θ_2 . The actuators provide feedback on the servo position, so the full position of the adaptive fingers can be estimated. This way, proprioceptive joint sensors provide information about the final gripper position that is related to the shape and size of the grasped object, without the need of external contact or force sensors.

Miniature potentiometers from *muRata* (model SV01 $10k\Omega$ linear) have been used successfully for the measurement of the distal joints of both fingers (θ_{2l},θ_{2r}). The analog signals are measured using a micro-controller with 10-bits ADC, (0.26° resolution) at a rate of 50Hz.

The *Dynamixel MX-28* servos have a magnetic encoder with 12-bits (0.088° resolution) at a rate of up-to 50Hz with our current set-up. They provide feedback of the servo positions θ_{al} and θ_{ar}.

[1]/github.com/TaISLab/umahand

C. Grasping forces

The forces at the center of the phalanxes contact areas in an underactuated gripper depends also on the joint values. Moreover the spring stiffness [18] is also in the equation.

$$f = J^{-T} T^{-T} t \tag{1}$$

Where f are the contact forces, T^{-T} is the inverse of the transposed Jacobian matrix that relates the finger joint velocities to the speed of the contact points, and T is the transfer matrix, that relates the velocities of the actuators to the joint velocities. Both matrices depends on the joints and actuator positions [17]. However, if the same final grasping position ($\theta_1 = 62.8^\circ, \theta_2 = 81.3^\circ$) is kept, the magnitude of the closing force of each finger ($f_1 + f_2$) is proportional to the actuator torque θ_a. Closing forces have been experimentally measured for different actuator torques at the same grasping position. With a maximum stall torque for each of the *Dynamixel MX-28* servos of 2.5 Nm, the effective closing forces for each finger range from 4.9 N (20%) to 27.4 N (100%).

A grasping operation has been programmed as a constant-velocity trajectory for both actuators in opposite directions with a stiff proportional-only controller with programmable torque limits. When both actuator velocities ($\dot{\theta}_1, \dot{\theta}_2$) are null, the goal point is set to the current position, stopping the motion of the fingers.

D. Gripper design validation

To validate the suitability of this design for pHRI, the contact pressure distribution between the fingers and the human's upper forearm skin in different roll angles and different torques has been studied. For this purpose, a thin-film high-resolution pressure-sensor system from *TekScan* has been placed between the gripper and the left-side of the forearm, as shown in Figure 3. Note that this sensor has been used for evaluation of the contact forces and pressures and it will no longer be used for the roll angle estimation.

This study reveals that, when using this kind of grippers, not all the grasping angles are the same in terms of human comfort. A roll angle of 90° offers a smoother grasp. A torque of 1.15 Nm (46% of the maximum torque) that provides a closing force of about 11.76 N per finger has been selected as the closing torque for the experiments, because it has been considered by the volunteers as a firm and gentle grasp.

E. Getting ground-truth data

In order to obtain the ground-truth angular measurement of the human forearm, a device that includes an accelerometer has been implemented. The device is held by the human on their hand during the experiments. As the attitude of the robot gripper is known, the relative rolling angle of the human forearm with respect the gripper can be obtained and used as a reference data for training and performance evaluation of estimation methods.

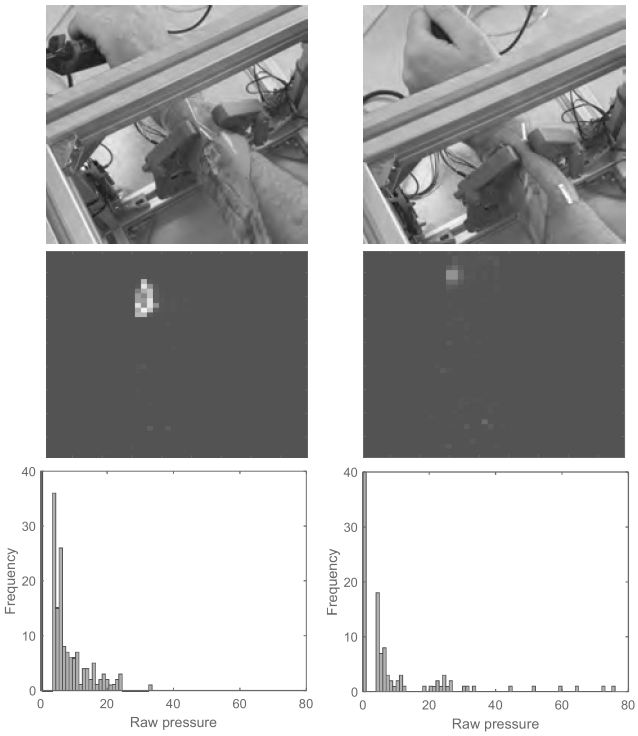

Fig. 3. Study of the pressure distributions on the human forearm for a rigid underactuated gripper with a high-resolution thin-film pressure-sensor showing images of the experiments (up), pressure images of the left-side of the forearm (middle) and histogram of the pressure images(down) for -45° (left column) and 90° roll angles (right column).

III. Forearm Roll Angle Estimation

The proposed method is based on the differences in the final grasping positions of the finger joints when grasping a human forearm, thanks to the internal bone structure, as seen in Figure 4. The human forearm is supported by Ulna and Radius, which specially at the upper section of the forearm (near the wrist) provide an elliptical shape. A roll angle (with respect to the gripper) is considered, when Ulna and Radius are parallel to the gripper base.

A. Measurements

During the measurements, the volunteer subject holds a 3D printed handle which integrates the accelerometer, while the gripper closes repeatedly around their forearm. This way, when the subject rotates the forearm, the accelerometer measures this rotation which corresponds to the roll angle. The whole gripper has been mounted on a square frame to perform experiments in different positions and extend the range of angular measurements. The actual roll angle is computed as the orientation difference between the gripper and the readings from the inertial sensor bar. This process is show in Figure 5, where the arm angle and joint values are recorded for a sequence of six grasps.

Performing many different grasps at different angles, the relationship between the gripper joints and the roll can be obtained. In Figure 6, the data of 36 grasps, measured at different angles, on the left arm of a volunteer with a perimeter of 17.9 cm, is shown.

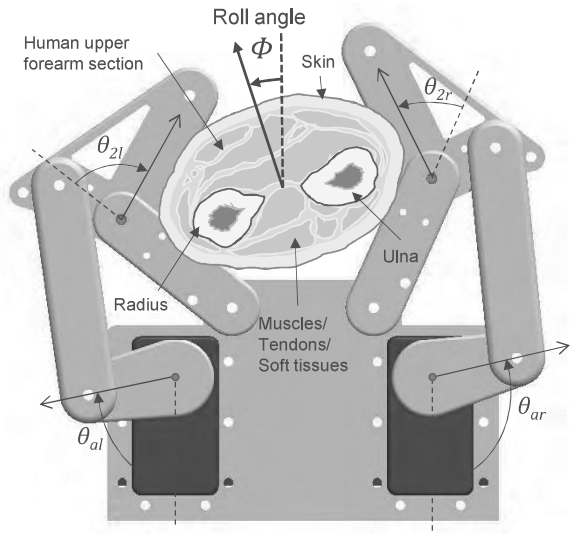

Fig. 4. Cross section of a human upper forearm grasped by the under-actuated gripper, showing the variations in the passive (θ_{2l},θ_{2r}) and active (θ_{al},θ_{ar}) DOF's, based on the roll grasping-angle (Φ).

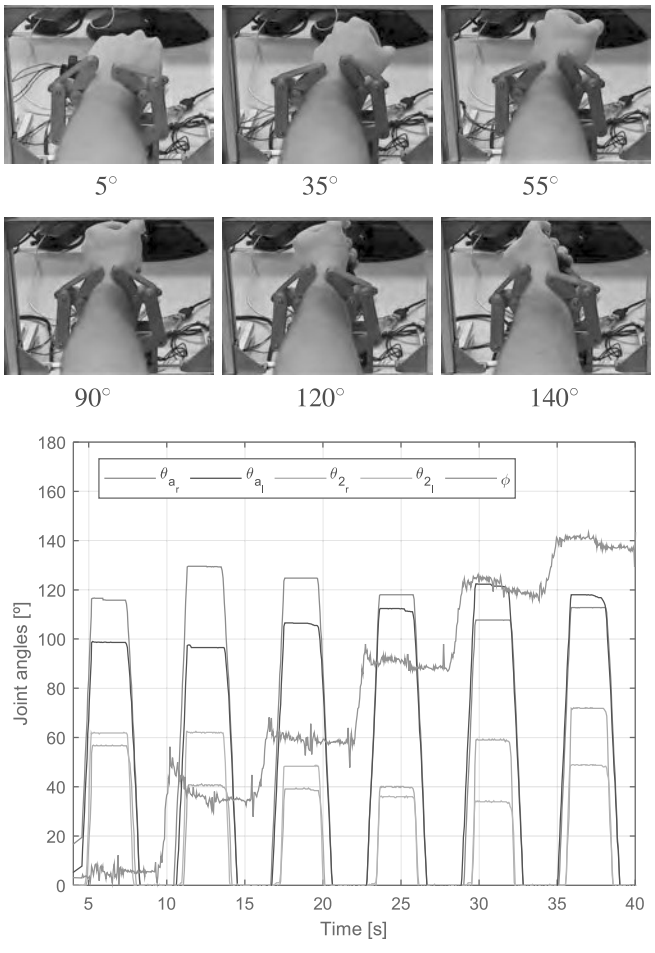

Fig. 5. Sequence of 6 grasps during the data collection process of one volunteer (top). Motors, joints and roll angle positions during a data collection process (bottom). Note that in this graph the open-and-close process is repeated each 6 s.

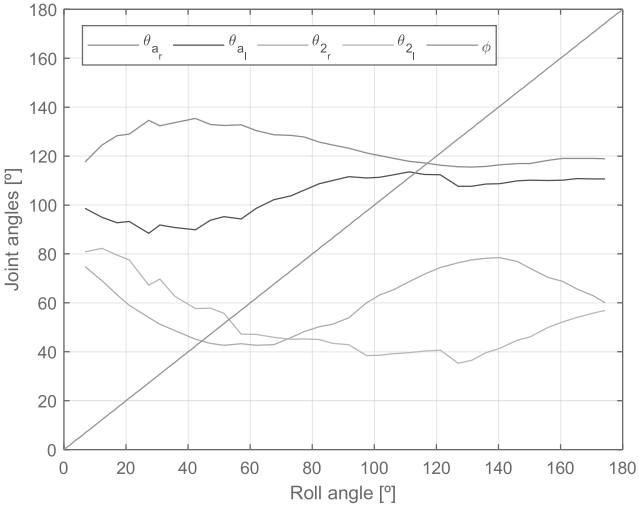

Fig. 6. Joint values for 36 grasps, measured at different angles, on the left arm of a volunteer with a perimeter of 17.9 cm, against the roll angle.

B. Machine-learning regression methods

To estimate the roll angle (ϕ), three machine learning approaches based on non-linear regression methods are used to obtain three models: Gaussian Process Regression (GPR) [19], Regression Tree (RT) [20] and Bagging Regression Tree (BRT) [21]. These models receive the 4-input angles $(\theta_{ar}, \theta_{al}, \theta_{2r}, \theta_{2l})$ and predict ϕ.

All these models are trained in a large dataset. In the training process, features are composed by sets of $(\theta_{ar}, \theta_{al}, \theta_{2r}, \theta_{2l})$, while expected responses composed by ϕ are measured with the accelerometer for each set of features. A cross-validation has also been included during the training process to prevent overfitting.

The training and evaluation processes have been carried out using *Matlab R2018b*, the *Statistics and Machine Learning Toolbox* and the *Regression Learner application*. The code and datasets have been made available in the repository referred in section II.

The training process have been carried out using the *Parallel Computing Toolbox* in a 4-core Intel i7-7700HQ CPU @ 2.80 GHz.

C. Data collection

During this process, a User Interface developed in Matlab shows goals and current angles so that the subject could rotate their forearm until goal and actual angle match. In each step, the gripper opens and closes, so while the gripper is closed, $(\theta_{ar}, \theta_{al}, \theta_{2r}, \theta_{2l})$ and (ϕ) values are collected.

There are two types of data collection processes which have been performed: sequential and random. In the sequential process, the subject is asked to rotate their arm in steps of 5°. In the latter, the goal angle is set randomly.

Following this process, two data-sets have been collected: the first dataset contains information of a single subject, while the second dataset contains information of five subjects. To train and test the models, each dataset is split into training and test sets respectively. Therefore, training and test

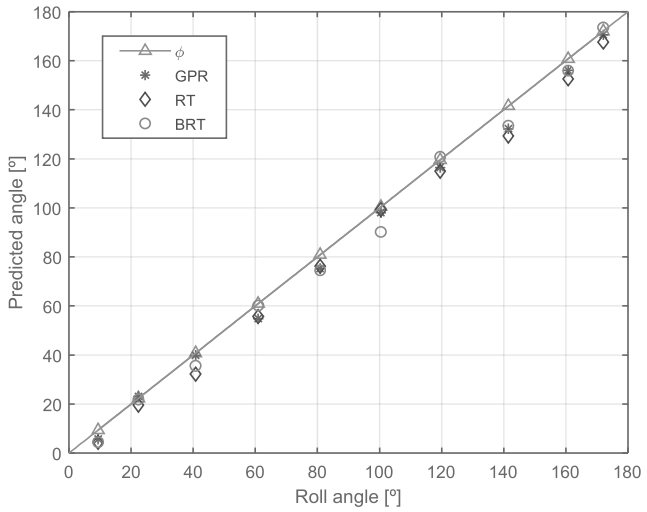

Fig. 7. Regression results of non-trained data of a known subject when models are trained in this subject dataset only.

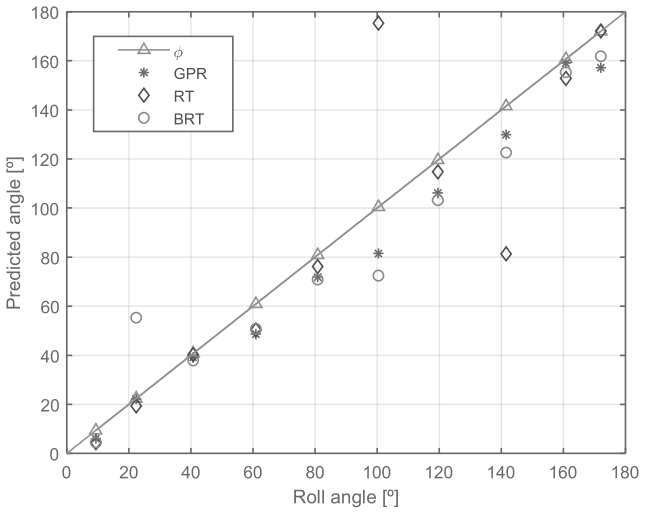

Fig. 8. Regression results of non-trained data of a known subject when models are trained in a dataset obtained from 4 volunteers.

data are different, even if they have been collected from the same person.

The dataset collected from one subject contains an amount of 555 sets of $(\theta_{ar}, \theta_{al}, \theta_{2r}, \theta_{2l})$ and (ϕ), while the dataset collected from 5 subjects is composed by 2775 sets of data.

D. Results

Three experiments have been carried out to measure the performance of the regression models estimating the roll angle:

1) **Single-known:** Training and test sets contains data from one subject.
2) **Multiple-known:** Training and test sets contain data from four subjects.
3) **Multiple-unknown:** Training set contains data from four subjects and test set contains data from a fifth subject which is not used to train the models.

In the single-known experiment, machine learning models have been trained with data from a single volunteer and have tested with different data from the same subject. The results of this experiment are shown in Fig. 7. This figure shows the good performance of the regression models, with an almost negligible error, and the best results obtained by GPR.

In the multiple-known experiment, machine learning methods have been trained with data from 4 volunteers and have been tested with different data from one of these 4 subjects. In this case, predictions from RT and BRT include a pair of outliers, however the GPR model still presents a good performance as can be seen in Fig. 8.

In the multiple-unknown experiment, regression models have been trained with data from 4 subjects and tested with completely new data from a fifth volunteer that had not been used in the training process. Results of this experiment are presented in Fig 9 and show that RT and BRT are more robust that GPR because they generalize better, and the outliers predicted in the previous experiment vanish.

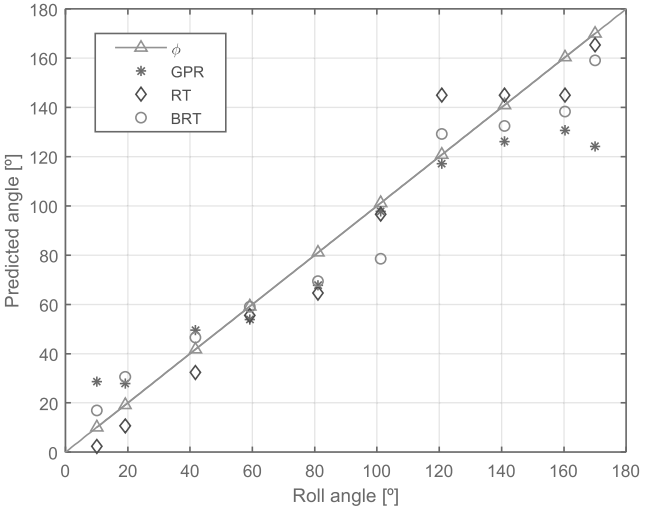

Fig. 9. Regression results (a) and errors (b) of non-trained data of an unknown user when models are trained in a dataset obtained from 4 people.

Results are summarized in Table II. The Maximum Erorr (ME) and Mean Absolute Error (MAE) from each model in each experiment are represented in degrees. As is commented before, GPR obtains the best results when the subject is known, with a MAE of 3.77° in the case of a single user and 8.68° in the case of multiple subjects. However, for the third experiment, the best results are achieved by the RT model with a MAE of 9.86° since this model generalizes better than the others. The maximum error shows the outliers in experiments

IV. Conclusions

With this method, new applications of robot-initiated pHRI can be developed without the need of external force/tactile sensors that are expensive or hard to deploy and maintain. These applications may include assistive, rescue or surgical robotics. With this approach, information on the location

TABLE II

SUMMARY OF REGRESSION MODELS ERRORS IN DEGREES

	Single-known		Multiple-known		Multiple-unknown	
Models	**ME**	**MAE**	**ME**	**MAE**	**ME**	**MAE**
GPR	9.24	3.77	18.89	8.68	45.79	15.09
RT	12.20	4.33	74.94	17.17	24.22	9.86
BRT	10.19	5.66	32.94	13.95	22.61	10.73

of the human limbs can be enhanced without the need of additional sensors.

Knowing the full location of the grasped objects is key in robotics and manipulation. In pHRI applications, an accurate location of the human forearm is important not only for a safe human arm manipulation, but also for the placement of biomedical devices such as heart-rate or glucose sensors. Although visual methods for the estimation of the location of human limbs provide the coordinates of the human joints (i.e. OpenPose), the roll information is not included. Moreover, the roll of the forearm may change during the grasping process.

The results demonstrate the good performance of the regression methods used in this application. The errors obtained denote these predictors can be used for pHRI applications. However, in future works, a larger dataset, and a greater number of volunteers may be considered, as well as the use of other prediction methods as deep learning.

Future works after this method may include forearm width estimation for the recognition of people, quality of grasping estimation and skin compliance identification for health evaluation.

REFERENCES

[1] K. Wada and T. Shibata, "Robot therapy in a care house-its sociopsychological and physiological effects on the residents," in *IEEE International Conference on Robotics and Automation (ICRA)*, 2006, pp. 3966–3971.

[2] M. Shiomi, K. Nakagawa, K. Shinozawa, R. Matsumura, H. Ishiguro, and N. Hagita, "Does a robots touch encourage human effort?" *International Journal of Social Robotics*, vol. 9, no. 1, pp. 5–15, 2017.

[3] S. A. Bowyer and F. R. y Baena, "Dissipative control for physical human–robot interaction," *IEEE Transactions on Robotics*, vol. 31, no. 6, pp. 1281–1293, 2015.

[4] Z. Li, B. Huang, Z. Ye, M. Deng, and C. Yang, "Physical human-robot interaction of a robotic exoskeleton by admittance control," *IEEE Transactions on Industrial Electronics*, 2018.

[5] A. Stilli, A. Cremoni, M. Bianchi, A. Ridolfi, F. Gerii, F. Vannetti, H. A. Wurdemann, B. Allotta, and K. Althoefer, "Airexglove - a novel pneumatic exoskeleton glove for adaptive hand rehabilitation in post-stroke patients," in *IEEE International Conference on Soft Robotics (RoboSoft)*, 2018, pp. 579–584.

[6] C. King, T. L. Chen, A. Jain, and C. C. Kemp, "Towards an assistive robot that autonomously performs bed baths for patient hygiene," in *IEEE/RSJ International Conference on Intelligent Robots and Systems (IROS)*, 2010, pp. 319–324.

[7] K. Chow and C. C. Kemp, "Robotic repositioning of human limbs via model predictive control," in *Robot and Human Interactive Communication (RO-MAN), 2016 25th IEEE International Symposium on*. IEEE, 2016, pp. 473–480.

[8] Z. Erickson, H. M. Clever, G. Turk, C. K. Liu, and C. C. Kemp, "Deep haptic model predictive control for robot-assisted dressing," in *IEEE International Conference on Robotics and Automation (ICRA)*, 2018, pp. 1–8.

[9] C. Yang, C. Zeng, P. Liang, Z. Li, R. Li, and C.-Y. Su, "Interface design of a physical human-robot interaction system for human impedance adaptive skill transfer," *IEEE Transactions on Automation Science and Engineering*, vol. 15, no. 1, pp. 329–340, 2018.

[10] J. Armendariz, R. García-Rodríguez, F. Machorro-Fernández, and V. Parra-Vega, "Manipulation with soft-fingertips for safe phri," in *Proceedings of the seventh annual ACM/IEEE international conference on Human-Robot Interaction*. ACM, 2012, pp. 155–156.

[11] A. H. Memar, N. Mastronarde, and E. T. Esfahani, "Design of a novel variable stiffness gripper using permanent magnets," in *IEEE International Conference on Robotics and Automation (ICRA)*, 2017, pp. 2818–2823.

[12] J. M. Gandarias, J. M. Gómez-de Gabriel, and A. J. García-Cerezo, "Human and object recognition with a high-resolution tactile sensor," in *IEEE SENSORS*, 2017, pp. 1–3.

[13] J. M. Gandarias, J. M. Gómez-de Gabriel, and A. J. García-Cerezo, "Enhancing perception with tactile object recognition in adaptive grippers for human–robot interaction," *Sensors*, vol. 18, no. 3, p. 692, 2018.

[14] L. Birglen, "Enhancing versatility and safety of industrial grippers with adaptive robotic fingers," in *IEEE/RSJ International Conference on Intelligent Robots and Systems (IROS)*, 2015, pp. 2911–2916.

[15] R. R. Ma, L. U. Odhner, and A. M. Dollar, "A modular, open-source 3d printed underactuated hand," in *IEEE International Conference on Robotics and Automation (ICRA)*, 2013, pp. 2737–2743.

[16] A. J. Spiers, M. V. Liarokapis, B. Calli, and A. M. Dollar, "Single-grasp object classification and feature extraction with simple robot hands and tactile sensors," *IEEE transactions on haptics*, vol. 9, no. 2, pp. 207–220, 2016.

[17] L. Birglen, T. Laliberté, and C. M. Gosselin, "Underactuated robotic hands." Springer, 2008, vol. 40.

[18] L. Birglen and C. Gosselin, "Optimal design of 2-phalanx underactuated fingers," in *Proceedings of the 2004 International Conference on Intelligent Manipulation and Grasping*, 2004, pp. 110–116.

[19] C. K. Williams, "Prediction with gaussian processes: From linear regression to linear prediction and beyond," in *Learning in graphical models*. Springer, 1998, pp. 599–621.

[20] L. Breiman, "Classification and regression trees." Routledge, 2017.

[21] L. Breiman, "Bagging predictors," *Machine learning*, vol. 24, no. 2, pp. 123–140, 1996.